X-ray Photoelectron Spectroscopy Study of Styrene Oxidation

Niclas Johansson

Bachelor Thesis

Fysicum, Division of Synchrotron Radiation Research
Lund University

LUNDS UNIVERSITET

Abstract

Silver has been proved as a heterogeneous catalyst for styrene epoxidation via detection of reaction fragments. After dosing styrene to the surface, reaction fragments were identified by comparing with literature values. The fragments were the oxametallacycle of styrene, carboxylic groups, benzene, and carbon residuals. The used surface were composed of a Pt(111) substrate, a one monolayer thick FeO(111) film, and oxidized Ag clusters. It was found that x-ray photoelectron spectroscopy alone is not sufficient to fully investigate the reaction. In this work the basic theory is given, the experimental methods and setup are described in some detail.

Contents

1 Introduction

The oxidation of ethene is an important and common chemical reaction. The worldwide demand of ethene in 2006 was 18 million tons [1]. Although widely used, the mechanism of this oxidation is poorly understood. Considerable effort has been put into the understanding of ethene epoxidation, but the reaction mechanism is unclear. To fully understand the reaction, one has to understand the reaction pathways and the reaction intermediates [2]. It is difficult to perform epoxidation experiments on ethene due to its weak adsorption to e.g. Ag, even if oxygen is present. When performing measurements in ultrahigh vacuum (UHV), ethene will desorb from a Ag surface at low temperatures [3]. To study the epoxidation of ethene one has to use other molecules that has similar structure; one of the molecules, which can be used is styrene. Styrene consists of a benzene ring with an ethylene group attached; it is the ethylene that is oxidized in the epoxidation reaction. Studies have shown that styrene oxidation in UHV conditions is a good model for studying ethene oxidation [4]. Styrene epoxidation itself is a used chemical reaction, therefore, styrene is ideal for studying epoxidation. In figure 1 the styrene molecule and a schematic view of epoxidation is shown. The reaction

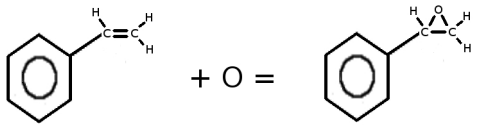

Figure 1: The styrene molecule and basic concept of styrene epoxidation

path of styrene epoxidation suggested by ref. [2] is shown in figure 2.

Styrene dosed to a surface is expected to form an oxametallacycle [2]. The oxametallacycle then either may react to styrene oxide or it might be combusted when heated. The combustion intermediate then forms benzoate. Benzoate may then form phenyl and CO_2. In the last step, phenyl forms benzene and biphenyl.

Metal oxides are involved in many areas such as biology, electrochemistry, and chemical sensing. One of the most important uses of metal oxides is as a heterogeneous catalyst [5]. To construct a heterogeneous catalyst, one uses a support and then forms clusters on this support. These metal oxide clusters are then used to synthesize organic compounds by selective oxidation, dehydrogenation and other processes. In catalysts, metal oxides are also often used as supports. Pure transition metals are also important as catalytic agents; platinum is often used [6] in various catalytic reactions and silver is

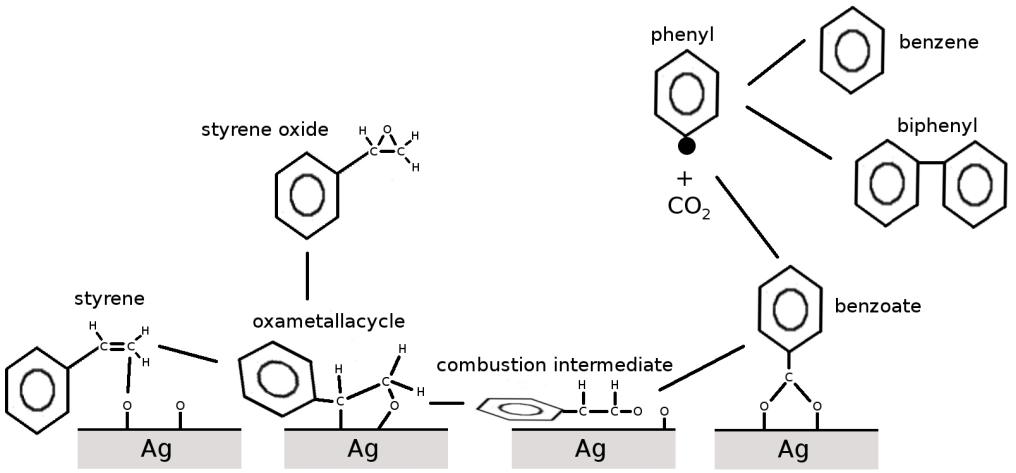

Figure 2: The reaction path suggested in ref. [2]

being used increasingly. When a thin FeO film is grown on a Pt substrate, the surface orients itself in such a way that it will be O-terminated [5]. Studies done by Weiss and Ranke [5] show that a surface constructed in this fashion will be inert to styrene. By using an inert surface as support, it does not interfere with the reaction. Due to this, the reaction is concentrated to the catalytic agent.

To study the oxidation of styrene, a Pt(111) substrate has been used here. On the Pt crystal, a thin FeO(111) film was grown. On the FeO film, Ag clusters were deposited and oxidized. The surfaces of the oxidized Ag clusters offer the possible binding sites for styrene. Earlier studies on styrene oxidation over silver have been made on silver single crystals. This experiment will deduce if it is possible to oxidize styrene utilizing clusters instead of entire surfaces.

2 Background

2.1 X-ray Photoelectron Spectroscopy (XPS)

The phenomenon of photoemission was first observed by Heinrich Hertz in 1887 [7] and later, in 1905, explained by Albert Einstein, for which he was awarded the Nobel prize in 1921. The basic principle of photoemission, which is illustrated in figure 3, is that a photon hits a material and excites an electron in such a way that it escapes from the material which it originally is bound to.

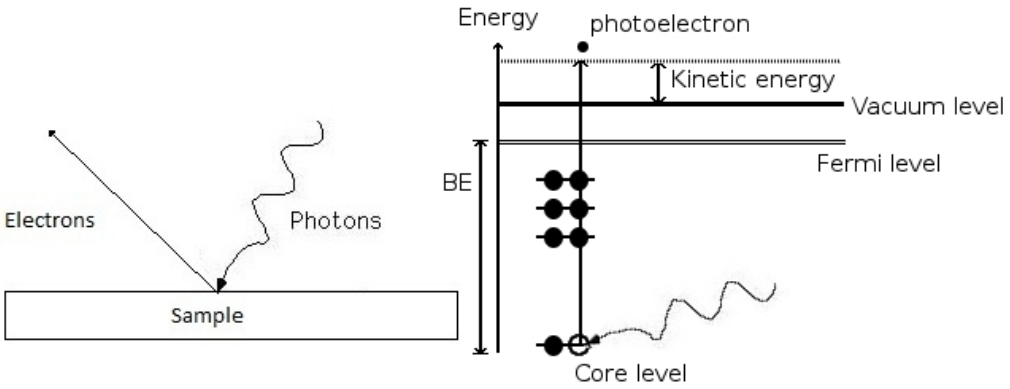

Figure 3: Left image shows an incoming photons that ejects an electron. Right figure shows an energy diagram of the process.

The emitted electron is called a *photoelectron* [7]. To produce a photoelectron, the incoming photons must have an energy greater than the work function, ϕ, for the surface through which the electron is emitted. The work function is defined as the minimum energy required to remove an electron from a solid through a particular surface [8]. By utilizing Einstein's photoelectric equation together with the principle of energy conservation, one can determine the kinetic energy of the photoelectrons:

$$E_{KIN} = h\nu - (E_B + \phi), \tag{1}$$

where E_{KIN} is the kinetic energy of the electrons, $h\nu$ is the photon energy, and E_B is the binding energy of the electrons. The energy available is the photon energy, thus it is clear that the kinetic energy will be the photon energy minus binding energy and work function. From Eq. (1) it is clear that a fixed photon energy and photoemission from well-defined atomic levels will yield kinetic energies unique to the element [8]. In solids, the valence levels,

the high-lying atomic orbitals, will participate in the bonding. By probing the core levels, which do not participate in the bonding, one can identify specific elements. Due to this, XPS is often called electron spectroscopy for chemical analysis (ESCA)[8].

Eq. (1) can be rewritten to:

$$E_B = h\nu - E_{KIN} - \phi. \tag{2}$$

From Eq (2) it is trivial to convert the measured kinetic energy into binding energy if the photon energy and work function are known.

When plotting photoelectron spectra it is convention to have increasing binding energy to the left, which means that kinetic energy increases to the right. In figure 4 on can see an example of a x-ray photoelectron spectrum of Pt 4f of a Pt(111) surface.

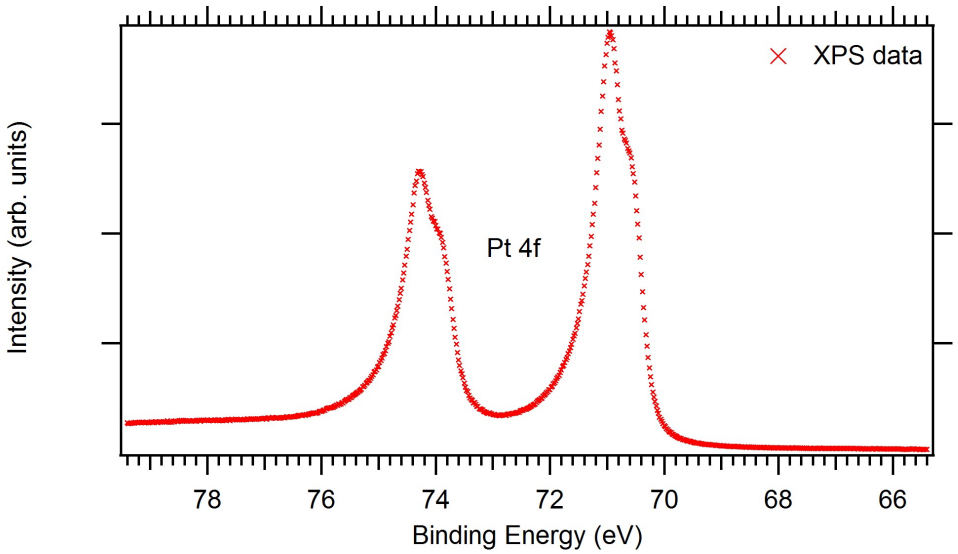

Figure 4: Example of an XPS spectrum. This is a spectrum of the Pt 4f core level of a Pt(111) surface.

It is often not of interest to investigate the absolute binding energies of solids, it is more interesting to observe how this binding energy changes due to the chemical environment, i.e. studying *chemical shifts* [7]. In a much simplified initial state picture; when molecules form, charge transfer may be induced. This may leave atoms with partial positive or negative charges [8]. These transfered charges will lead to a change in coulomb interaction between the core electrons and the nucleus which will create shifts in binding energy. By observing the chemical shifts it is possible to determine how, and possibly what the observed element has bound to.

The reason for using XPS in surface science is its surface sensitivity. When electrons are traveling through matter, they scatter. Inelastically scattered electrons lose energy. The electrons of primary interest are those that have not yet scattered, or scattered elastically. The mean distance inside matter that electrons can travel without loosing energy is called the *mean free path*. For condensed matter, the mean free path is only a few Å long [7]. The thickness of atomic layers are in the same magnitude as the electron mean free path, meaning that only photoelectrons from the topmost layers will escape without losing energy. When only the topmost layers contribute to the peak, the technique is surface sensitive. The electrons from the bulk scatter multiple times and build up the background.

2.2 Synchrotron Radiation

A synchrotron is a circular particle accelerator. Classically, a charge under acceleration emits radiation with the dipole distribution, $sin^2\theta$, where θ is the angle between the direction of the radiation and the field. At low speeds, electrons in a curved path will emit radiation with the dipole emission pattern [9]. In electron storage rings, the electrons are kept at a speed close to the speed of light, c. When the electrons approaches c, their emission pattern will change due to relativistic effects. Instead of the dipole distribution, the radiation will be emitted in a cone-shaped pattern in the electron forward direction with a cone opening angle inversely proportional to the electron energy [9]. The opening angle is typically a small fraction of a degree and the light will be linearly polarized in the electron trajectory plane.

The short sweep time for an electron emission lobe over the detector, orbit and energy fluctuations, smears out the energy distribution. The radiation emitted from a electron storage ring covers a very large energy range, due to the smearing out, the radiation extends into very low energies [9].

To improve performance of a synchrotron, undulators are used. An undulator is a an array of magnets with periodic change in polarity, this will make the electrons take a sinusoidal path. This sinusoidal path will create more bends, and the electrons will emit radiation at each bend. The emitted radiation will self-amplify due to interference and the intensity will be greatly improved [9].

A synchrotron radiation facility is dedicated to extract radiation from the electrons. This experiment was carried out at the synchrotron radiation facility MAX-lab, at the MAX-II electron storage ring. The MAX-II electron storage ring is a 1.5 GeV third generation storage ring optimized for soft X-rays and very ultraviolet radiation [10].

2.3 Some Basics from Solid State Physics

A crystal is a periodic three dimensional array of the same building blocks that may include impurities and imperfections [11]. When defining the crystal structure, one speaks of the basis and lattice points. An ideal crystal is constructed by infinitely repeating an identical group of atoms. This group is called the *basis*, and the associated points in space are called *lattice points* [11]. The number of atoms in the basis may be one or more depending on the material. The lattice points are mathematical tools and for each lattice point one will have a base at that position. The central position of an atom in the basis relative to origin is:

$$r_j = x_j a_1 + y_j a_2 + z_j a_3, \tag{3}$$

where a_1, a_2, a_3 are the unit vectors and x_j, y_j, z_j are integer numbers. For every combination of a_1, a_2, a_3 there will be a lattice point. The origin may be chosen as any lattice point in the structure associated with the basis. Using the above reasoning one can construct 14 types of three dimensional lattices [11]. In figure 5 three of these are shown.

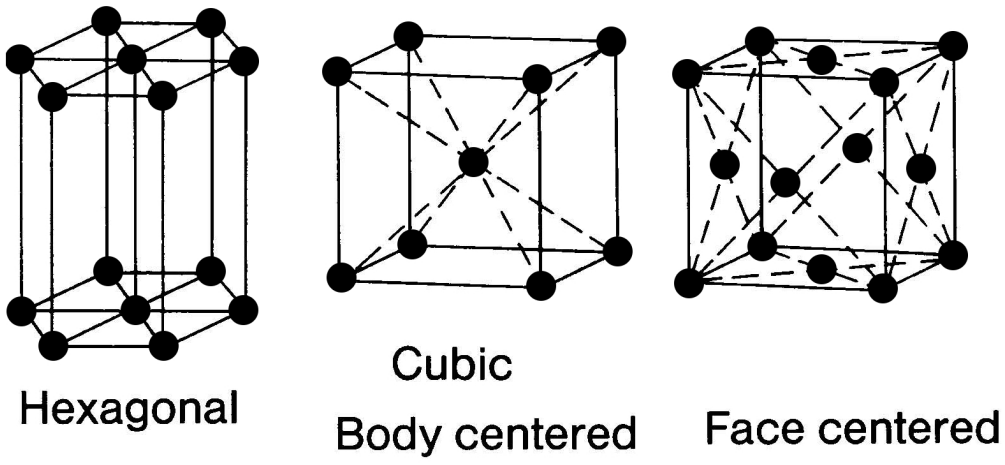

Figure 5: Three of the fourteen lattices. These three are most significant for solid state physics.

The most important lattices for solid state physics are the hexagonal, and the two centered cubic lattices [12]. The one interesting in this project is the face centered cubic(FCC) lattice. In surface science one works with surfaces and not the bulk structure, this means that one will have to cut the crystal. This is described by the *miller indices*. Depending on how one cuts a crystal, different surfaces will arise. These different surfaces have different properties

so it is important to know which surface one has. The normal of a plane is unique to the associated surface, therefore, the normal of the plane is used to designate the surfaces. The plane in fig. 6a has a normal equal to (111). Therefore the surface in 6a is called a FCC(111) surface. This creates the surface seen in figure 6b.

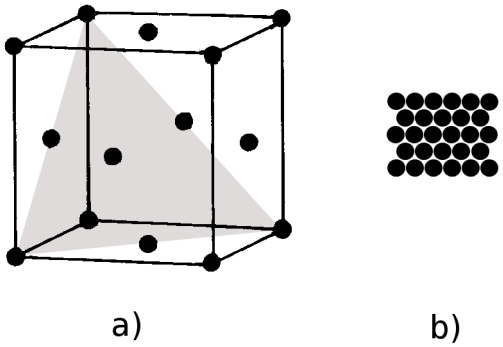

Figure 6: a), the shadowed area represents the (111) plane b), top view of the plane in b).

The coverage on a substrate by adatoms is described by monolayers. There are different definitions of what a monolayer is. One of those are that a monolayer (ML) is the amount of atoms it takes to occupy all available sites for that specific atom on a substrate. When dosing gases onto surfaces, pressure and time determines the amount of gas the surface is exposed to. The unit used for stating gas amounts is Langmuir(L). 1 L is defined as $10^{-6} Torr\ s$ [3]. In Europe, mbar is often used instead of Torr, therefore 1 L=$1.33 \cdot 10^{-6} mbar\ s$.

3 Experimental Setup

3.1 Beam line

The experiment was conducted at beam line I311 at MAX-lab. Beam line I311 is a soft x-ray beam line, constructed for high resolution electron spectroscopy [13]. The photon energy ranges from 30 eV up to 1500 eV that can be chosen according to element of interest. The monochromator at I311 consists of a plane mirror and a single grating, resulting in a high resolving power [13]. The exit slit from the monochromator has a fixed position, but the width may be changed. Figure 7 shows a schematic layout of beam line I311.

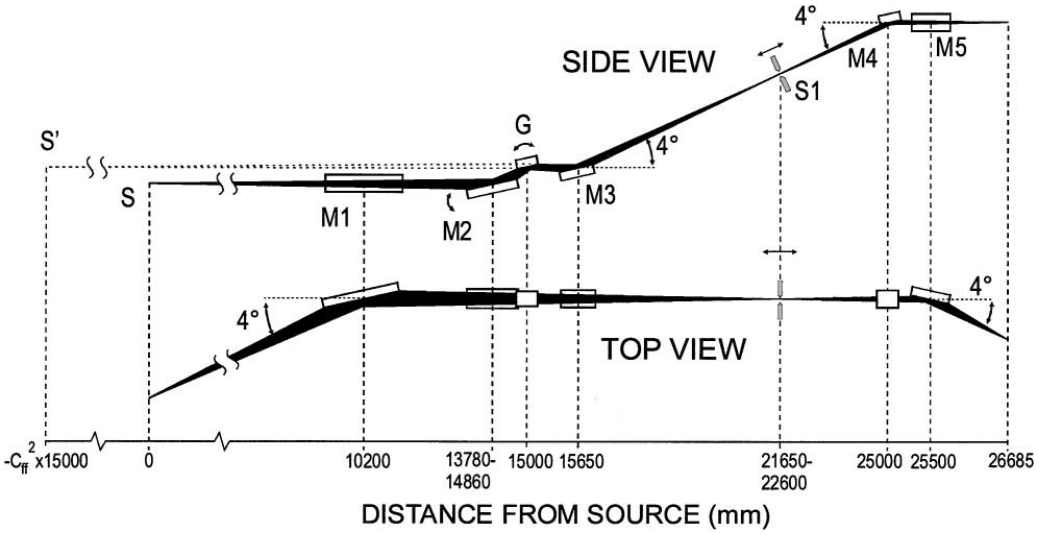

Figure 7: A schematic view of beamline I311. The optical components are: M1 is a horizontally focusing pre-mirror; M2 a rotable plane mirror, G the plane grating of the monochromator; M3 a spherical focusing mirror; M4 and M5 are spherical re-focusing mirrors. S is the real light source and S' is the virtual monochromatic source. S1 is a movable slit. Image taken from [13].

The beamline consists of: a horizontally focusing pre-mirror; a rotatable plane mirror, a plane grating, a spherical focusing mirror, and two spherical re-focusing mirrors

3.2 End Station

The end station at I311 consists of an analysis and a preparation chamber; the preparation chamber is mounted on top of the analysis chamber. The sample is moved between the chambers using a vertically mounted long-travel manipulator. Stationary equipment on the end station include a sputtergun, a gas dosing system, and an electron energy analyser. For the experiment, the

end-station was fitted with evapoators. Figure 8 shows a schematic image of the evaporation process, the left figure shows evaporation by electron beam heating, and the right shows evaporation by resistive heating.

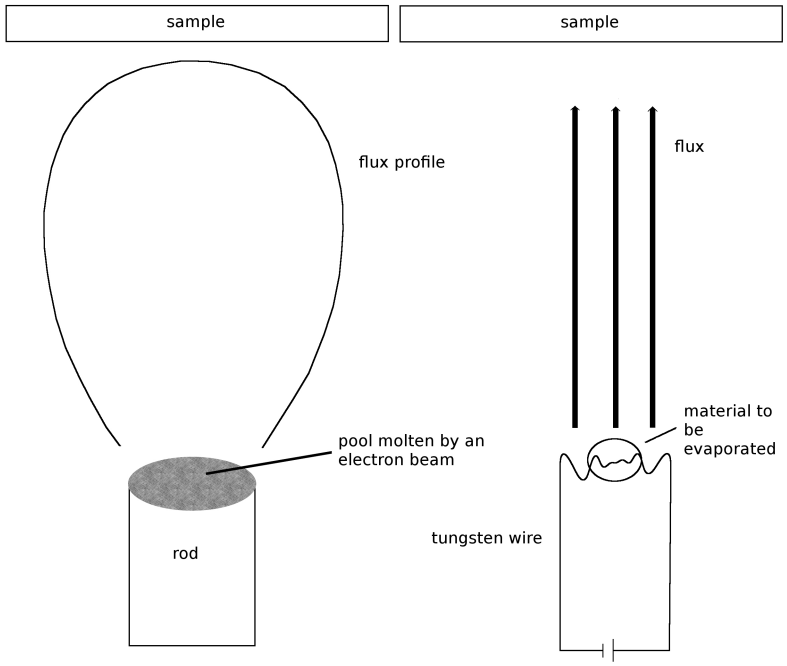

Figure 8: Schematic image of evaporation the evaporation process. The left image shows evaporation by electron beam heating, the right image shows evaporation by resistive heating. The flux is directed by electric fields.

In electron beam heating, a rod of a selected element is heated by an electron beam; the electrons are accelerated by high voltage. The heating results in ejection of ions from the rod. These ions will then condensate on the sample[14]. In resistive heating a wire is used to heat the material to be evaporated, in this case a tungsten wire. To direct the ions in the forward direction, an electric field is used. The evaporation is conducted in UHV conditions to minimize contamination of the sample. In this experiment, electron beam heating was used to evaporate Fe, and resistive heating was used for evaporating Ag.

An Ar sputtering gun was used for sputtering. Sputtering is a technique in which one bombards a surface with energetic particles, usually rare gases [15]. When energetic ions hit a surface, atoms on the surface will be ejected; this will clean but, roughen the surface. To get a smooth surface, one anneals it, which means heating the surface to a certain temperature and holding it at this temperature for a short time. When heating a surface, the surface atoms start to move, i.e. they diffuse, which smoothens the surface. When

annealing a surface, the temperature is kept constant for a short time. Another technique called to flash, is when one just raises the temperature to, e.g. 700 K and immediately stops the heating when the chosen temperature is reached.

The preparation chamber is constantly pumped by turbo pumps to get the pressure down to 10^{-8} mbar. The turbo pumps ran constantly even at gas dosing. To get the pressure down to 10^{-10} mbar, an ion pump was used.

3.3 Electron Energy Analyser

An electron energy analyser is used to detect the kinetic energy of the photoelectrons. An electron energy analyser consists of two concentric hemispheres with a potential difference between them. The potential between the hemispheres selects which energy an electron must have to pass through the detector, this is the pass energy, E_p. Electrons that are too fast will hit the outer hemisphere, the ones that are too slow will hit the inner hemisphere. Figure 9 shows a schematic image of an electron energy analyser.

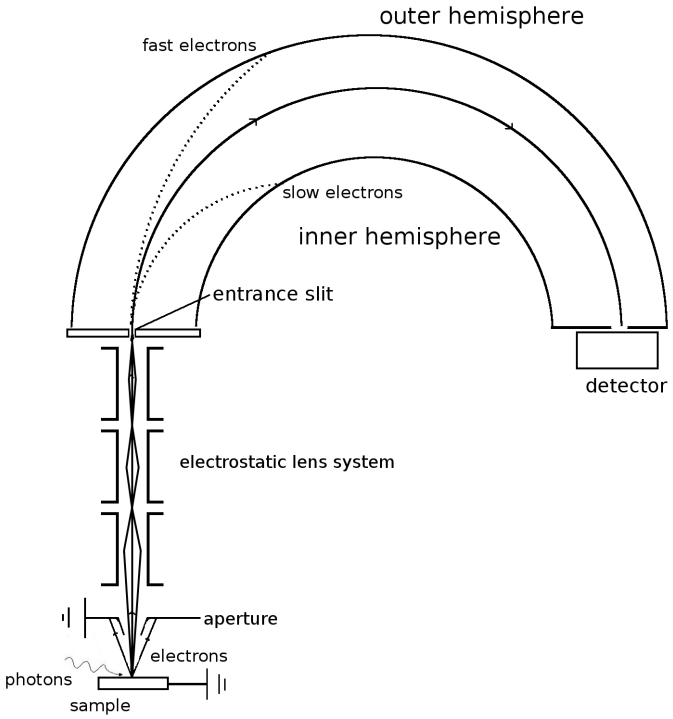

Figure 9: A schematic image of an electron energy analyser. Electrons are ejected from the sample, passing though an aperture. After the aperture the electrons pass through the electrostatic lenses. Then the electrons pass through the entrance slit to the detector if they have the correct energy.

An electrostatic lens system is used to increase the count rate, as well as manipulate the electrons [16]. The electrostatic lenses can either slow down or speed up electrons passing through. By sweeping the accelerating voltage applied to the lenses one can obtain a complete spectrum. The electron energy analyser used at beam line I311 is a Scienta SES200 analyser.

4 Methods

4.1 Calibration of the Evaporators

To calibrate the Fe evaporator, iron was deposited on the surface for different amounts of time. After iron had been evaporated on to the surface, it was oxidized.

Carbon monoxide does not bind to iron oxide, so by dosing CO one can see if 1 ML FeO is obtained by performing XPS measurements, looking for C 1s that has bound to Pt. When no C is detected, the FeO coverage is at least 1 ML. By probing at different points on the crystal, one can deduce the extensions of the FeO film. By knowing the position and extension of the FeO film, one knows where the silver should be deposited. Figure 10 shows the amount of C at different positions and at different cycles.

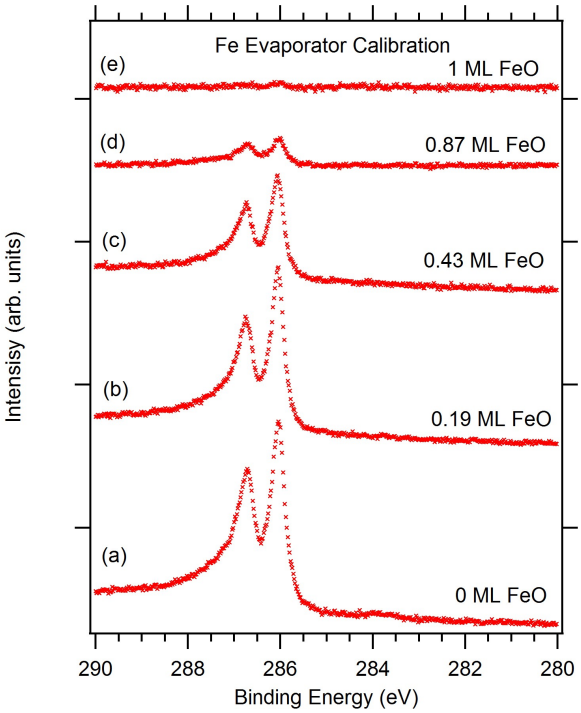

Figure 10: C1s XPS spectra at different Fe deposit cycles and positions. (a) shows the clean crystal, (b) after first deposition, (c) first deposition with a different position. (d) Second deposition. (e) third deposition and one ML is obtained.

After obtaining 1 ML FeO, the silver evaporator were to be calibrated. By taking spectra at different deposition cycles one can deduce for how long one should deposit Ag. In figure 11, different spectra of Ag 3d are shown, taken after different deposition times. One can see that increased deposition

time lead to increased amounts of Ag. In figure 11 a shift due to an increased Ag coverage can be seen.

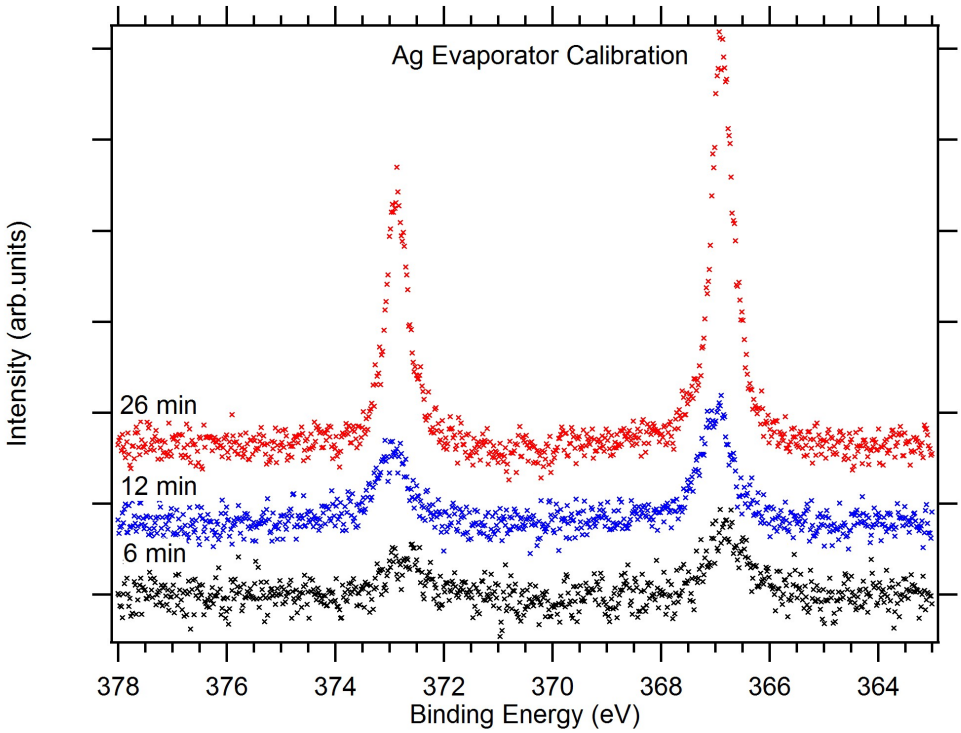

Figure 11: Ag3d spectra taken at different times, one can clearly see that with increased deposition time an increased amount of Ag is obtained on the surface. One can also detect a shift due to the larger amount Ag present at the surface.

4.2 Surface Preparation and Dosing of Styrene

The crystal was cleaned by repeated cycles of sputtering for 15 min and annealing at 930K for 5 min. The cleanness of the surface was controlled by XPS measurements. By taking an overview spectrum, the overall composition could be found.

Iron was deposited onto the clean crystal in two cycles of 10 min each. In between and after the deposition cycles, the crystal was oxidized by heating it up to 870 K in an oxygen-rich atmosphere of $1{\cdot}10^{-6}$ mbar pressure. Onto this FeO surface Ag was deposited for 20 minutes. The pressure during Ag deposition rose to $4 \cdot 10^{-10}$mbar. The silver was oxidized by dosing O_2 for 2 minutes at $4 \cdot 10^{-5}$mbar pressure.

Increasing amounts of styrene were dosed. The initial dose was 0.1 L, and subsequent doses were another 1 L, 10 L, 100 L, and finally 1000 L.

Measurements where taken in between every step. The surface was then flashed two times, first to 452 K and then to 701 K.

4.3 Data Analysis

The acquired data are uncalibrated. The electron energy analyser measures the kinetic energies of the incoming electrons, but the outcome will be affected by chosen settings such as pass energy and analyser slit. Changes in the contact potentials inside the analyser will occur, leading to additional changes. The problem of measuring kinetic energies is remedied by referring to the Fermi level, which aligns for the sample and analyser. Hence, by fitting a step function to the "Fermi edge", one can deduce the zero-point in the spectrum. When the zero point is found, the spectrum may be calibrated by shifting the data accordingly. In figure 12 one can see a spectrum of a Fermi energy with a fitted step function. The fit function shows that it is centered at -0.38 eV and thus by shifting all data +0.38 eV, the spectrum is calibrated.

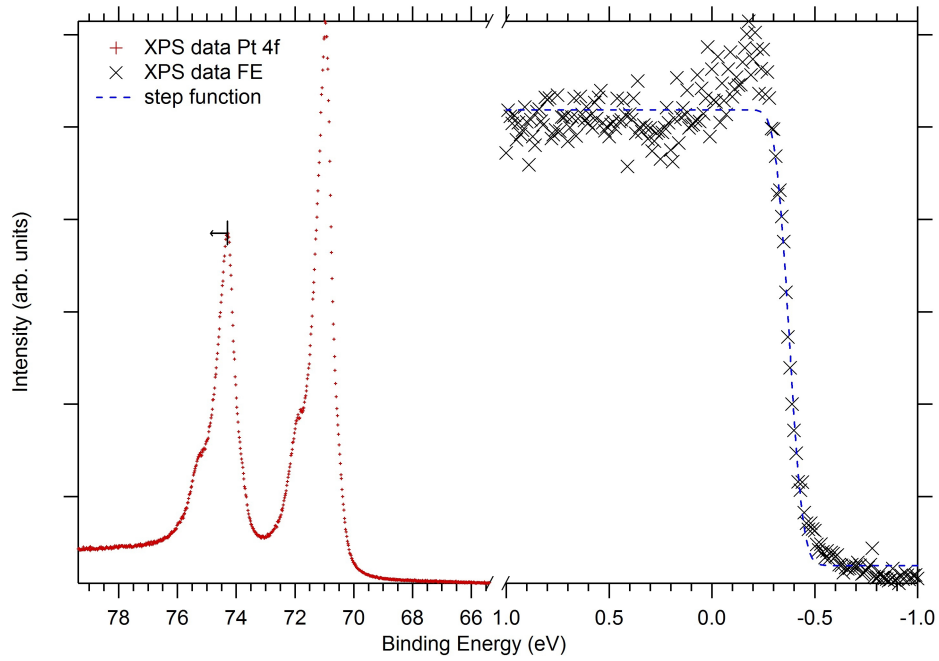

Figure 12: Spectra of the Fermi energy and Pt 4f. One can clearly see the step shape and that it is not at zero. The fitted step functions yields that the center of the Fermi energy is -0.38 eV, in the left image, it is shown in which direction the peak must be moved 0.38 eV to calibrate the spectrum.

For the Ag 3d and O 1s levels, Doniach-Šunjić line profiles were used for curve fitting. The curve fitting was performed with the FITXPS2 program.

When analyzing the C 1s spectra Igor Pro was used. Prior to fitting a polynomial background was removed, then Gauss functions were fitted to the C 1s peaks utilizing the global fit procedure. The global fit procedure can fit many spectra at the same time, using chosen parameters. In the C 1s fit, the FWHM for the "same" peaks were locked to be the same.

The resolution of a spectrum depends on photon energy, monochromator slit size, analyser slit size, pass energy of the analyser and the size of the analyser. The total resolution is a convolution of two different contributions, the monochromator energy resolution and the energy resolution of the electron energy analyser. The energy resolution of the analyser can be obtained from the following formula:

$$\Delta E_A = E_p \frac{W}{2R}, \tag{4}$$

where E_p is the pass energy, W is the slit width, and R is the radius of the analyser. The resolution of the monochromator, ΔE_M, is obtained from a graph available at ref. [17]. The total resolution is:

$$\Delta E = \sqrt{\Delta E_M^2 + \Delta E_A^2} \tag{5}$$

Different photon energies and pass energies are used for the different levels. All spectra were taken with the same monochromator slit size, 60 μm, and the same slit on the electron energy analyser, 0.8 mm. In table 1 the estimated resolution for the different spectra calculated from Eq.(5) is shown.

Table 1: Calculated values for the energy resolution obtained for the different spectra

Spectrum	$h\nu$ (eV)	E_p (eV)	ΔE_M (meV)	ΔE_A (meV)	ΔE (meV)
Fe3p	153	50	22	100	100
Pt4f	170	20	25	40	50
C1s	380	50	95	100	140
Ag3d	480	50	140	100	170
O1s	650	50	230	100	250
Overview	850	20	350	40	350

5 Results and Conclusions

5.1 Styrene Bonding

Figure 13 shows the Ag 3d spectra before and after oxidation. Curve fitting showed that the Ag 3d peak had shifted 0.04 eV towards higher binding energy meaning that the clusters indeed were oxidized. The O 1s spectra provided little information about the binding to silver, since it is strongly dominated by the O 1s signal from the FeO surface, as is shown in figure 14.

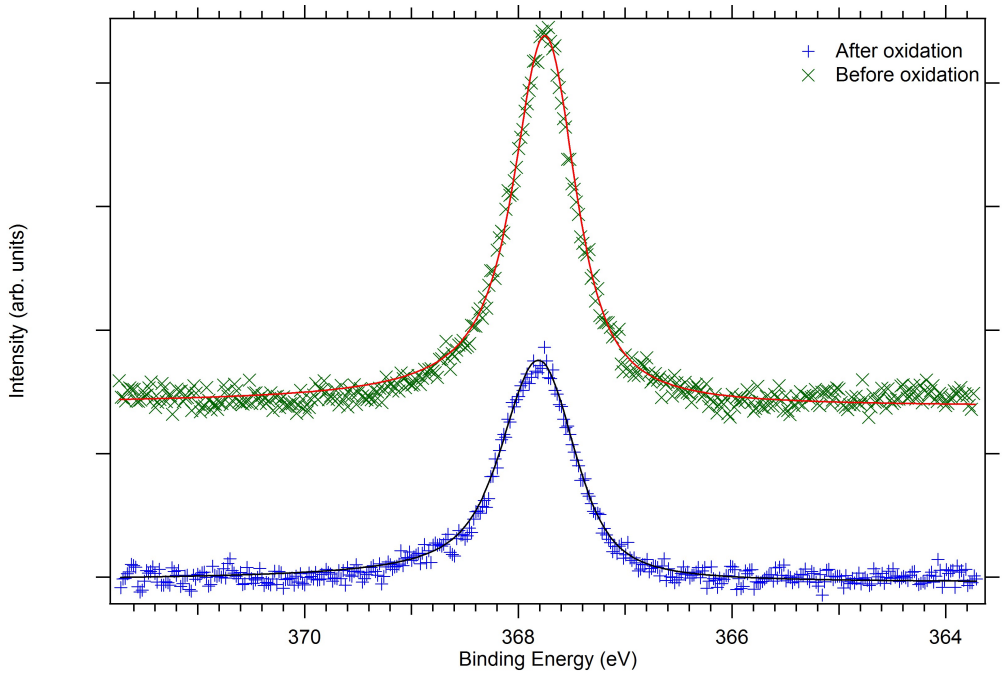

Figure 13: Spectra showing Ag 3d before and after oxidation. Curve fitting showed a shift of 0.04 eV. Polynomial backgrounds have been removed. The markers represent the data points and the lines are the fitted functions.

After dosing 10 L styrene, the Ag 3d peaks did not change. The change is simply too small for being detected, as seen in figure 15. Measurements on C 1s proved that styrene has bound at this dose (see figure 17).

Figure 16 shows Ag 3d spectra after an additional styrene dose of 100 L; now there are two peaks visible. This means that styrene did bind to the Ag clusters. Curve fitting performed on the Ag 3d peaks showed a binding energy shift of 0.26 eV for the main peak. The small peak had shifted 0.07 eV towards lower binding energy compared to the oxidized Ag 3d peak. Even higher styrene doses did not affect Ag 3d other than damping the signal, suggesting that one ML is reached. Due to the unaffected Ag 3d peak at 10

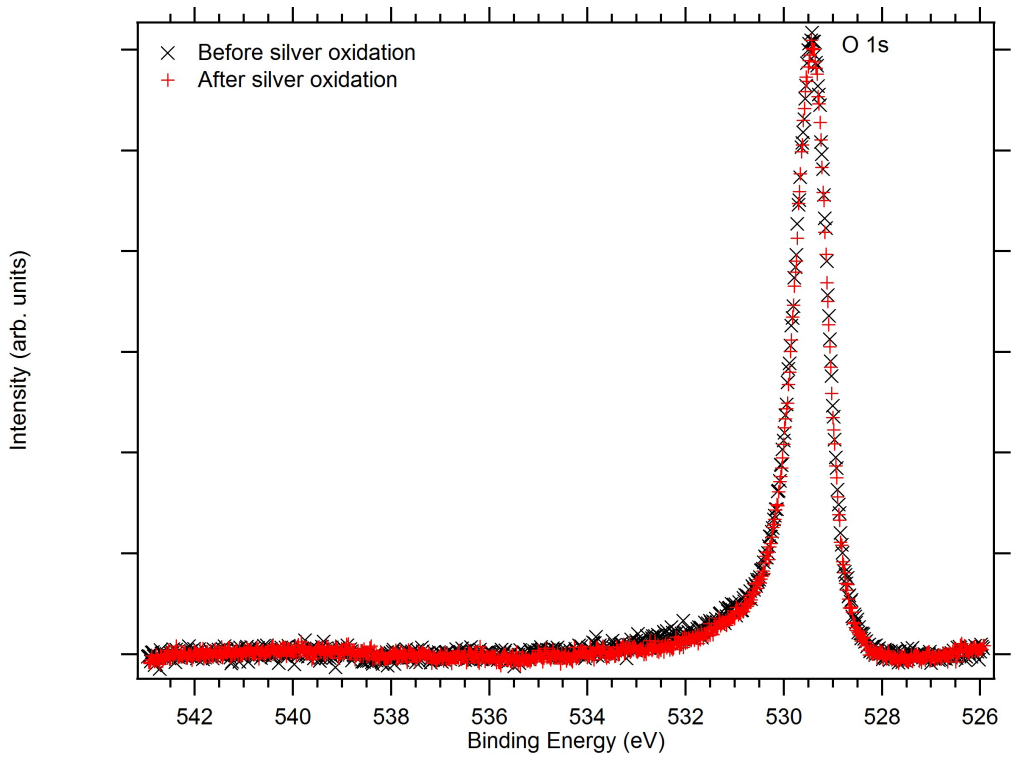

Figure 14: O 1s spectra, before and after oxidation of the Ag clusters. There is no visible change between the spectra which leads to the conclusion that the signal is too small and hidden by the O 1s signal from the FeO.

L, one can conclude that styrene has a low sticking coefficient.

The binding effect of styrene in O 1s can not be seen at low coverages. The O 1s signal from FeO hides the O 1s signal from the oxidized Ag. At this stage, it is uncertain whether the styrene did bind to the oxygen atoms. At higher coverages, it is still unclear if styrene did bind to O due to the unaffected peak. If one wants to see a change in O 1s, taking measurements at grazing angle might show a shift due to increased surface sensitivity.

It is obvious that styrene has bound to the silver clusters; according to ref. [18] styrene will bind to both Ag and O atoms. There are two situations possible, either the styrene did not bind to O on the Ag clusters, or the signal is just covered by the O from FeO. As mentioned above, complementary methods are required to further investigate the bonding to O.

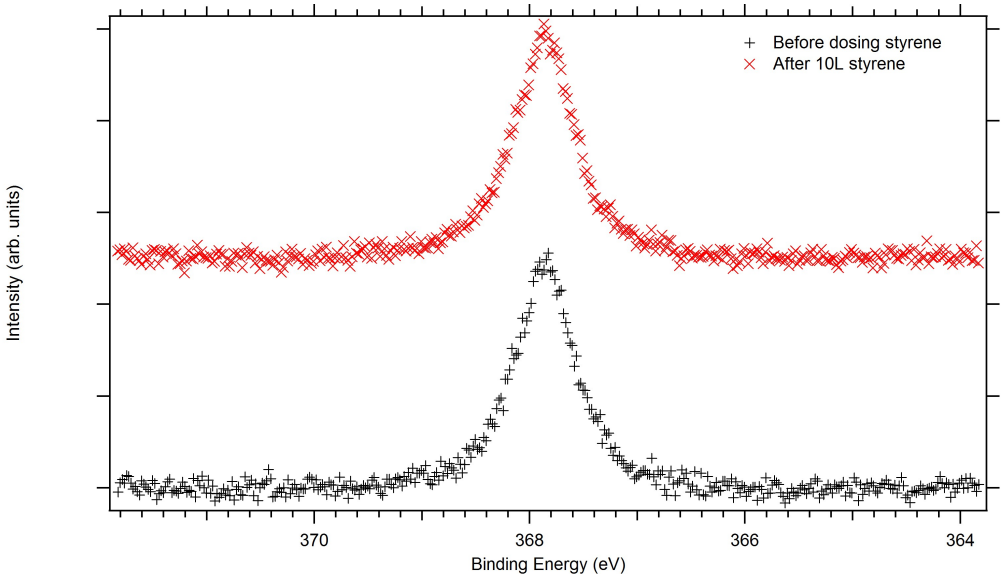

Figure 15: XPS spectra of Ag 3d before and after dosing of 10 L styrene. The two peaks are very similar and one can see that changes are small.

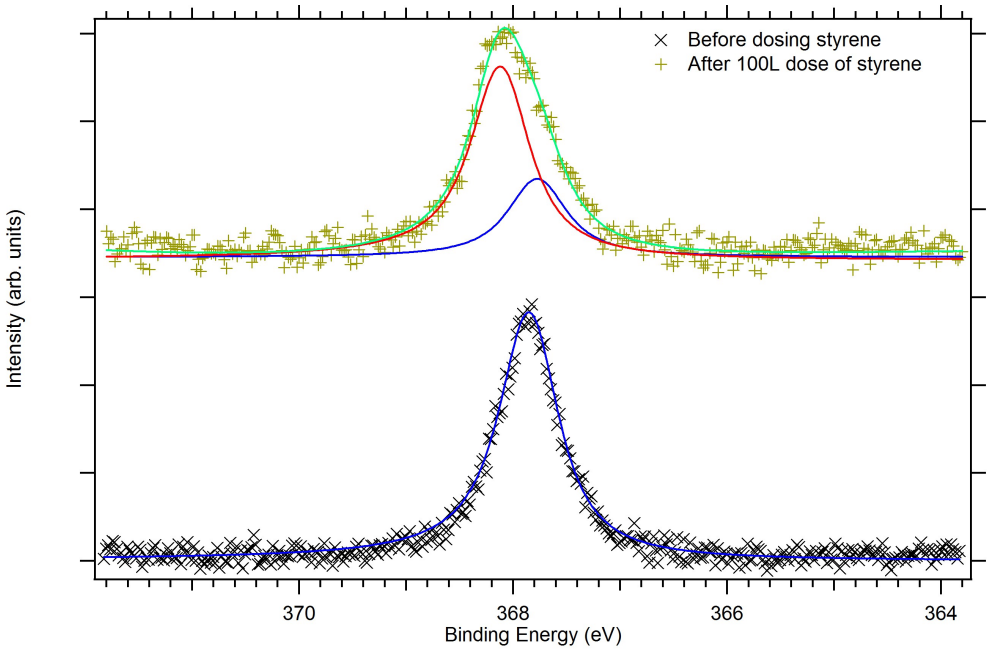

Figure 16: XPS spectra of Ag 3d before dosing styrene and after dosing 100 L styrene. In this spectrum one can see that the silver peak has split into two peaks, which proves that styrene has bound to the silver clusters. The lines in the spectra are the fit functions

5.2 Styrene

If the properties of styrene changes one will see this change in terms of binding energy changes in the C 1s spectrum. In figure 17 a spectrum of C 1s is shown after dosing 10 L styrene onto the sample. Due to the global fit used, three different peaks are detected showing that C has bound in three distinct ways.

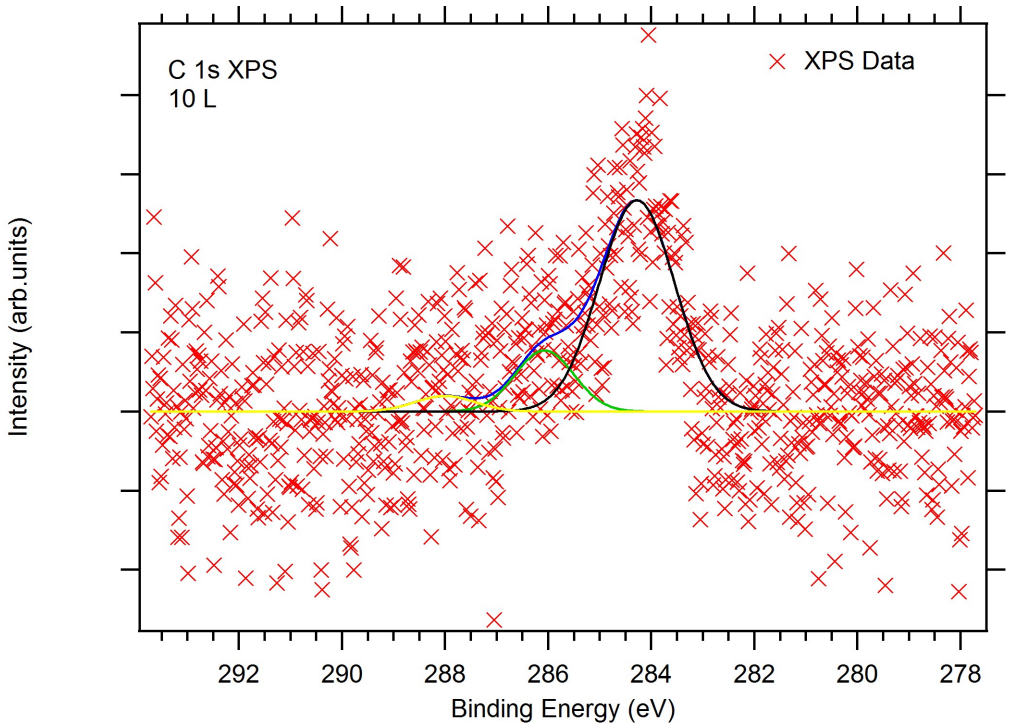

Figure 17: XPS spectum of C 1s after dosing 10 L styrene. One can see three peaks originating from C that is bound in three different ways. The signal is very small thus meaning that just a little styrene has bound to the surface. The lines are curve fits.

Binding energies and peak FWHM from spectra of C 1s for doses of 100 L, 1000 L, postflash to 452 K, and 701 K are presented in table 2. Figure 18 presents a C 1s spectrum for 1000 L styrene. One can assume that peak 3 originates from the benzene ring, due to the fact that it is the strongest of the three peaks; this assumption is supported by previous studies [2]. In ref. [2] it was found that an energy of 285.6 eV originates from the "non-phenyl" C in the oxametallacycle. Whereas in ref. [4] it was found that the oxametallacycle has a binding energy of 285.7 eV, a difference of 0.1 eV compared to ref. [2]. From this it is possible to attribute peak 2 to the oxametallacycle of styrene. Ref. [20] attributed a C 1s binding energy of 287.9 eV to carboxylic groups, a binding energy, which compares well to that

of peak 1. Therefore, peak 1 is attributed to carboxylic groups for the three first values in table 2. The carboxylic groups are suggested to originate from benzoate. Ref. [2] found a binding energy of 287.4 eV for the carboxylic group in benzoate, which is lower than the values obtained here. Therefore, no benzoate is detected.

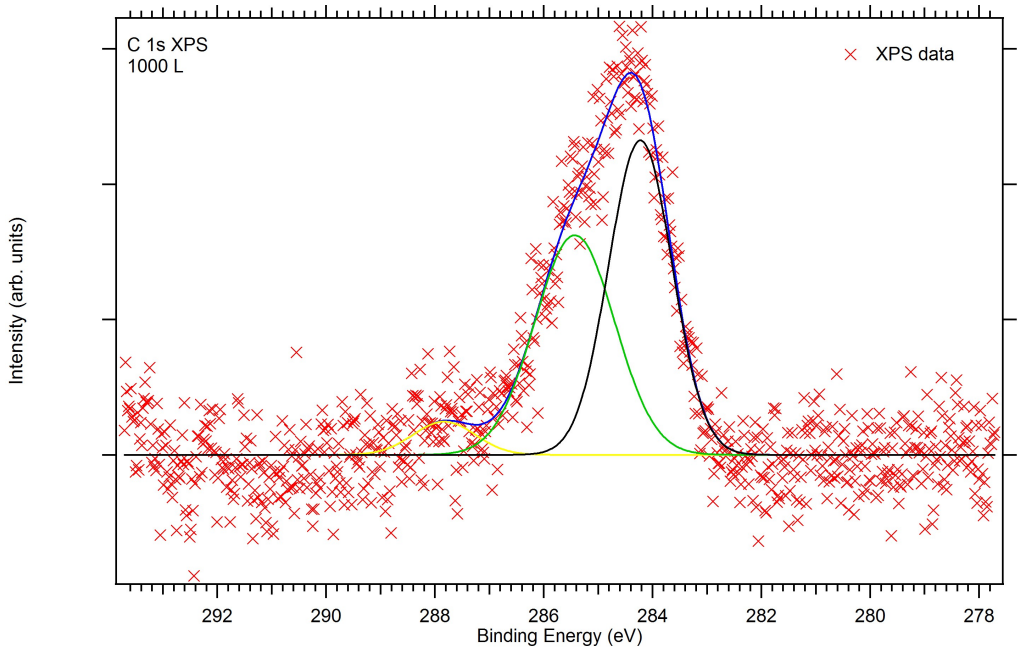

Figure 18: An XPS spectra of C1s after dosing 1000 L styrene. One can clearly see three distinct peaks corresponding to the three different "sorts" of carbon atoms in styrene. The lines are the fitted gauss functions.

Flashing the sample to 452 K resulted in slight spectral changes, see figure 19. The binding energies were not significantly shifted and the spectrum still has three peaks. Peak 1 has changed its binding energy with 0.17 eV towards higher binding energy, implying that one C atom underwent a change. The rest of the C 1s peaks appear to be unchanged. It is interesting to note that in figure 19 the unchanged peaks have changed their intensity ratios. Heating leads to desorption of the adsorbates. By flashing the surface, some of the styrene probably desorbed. The change in binding energy for peak 1 can thus be due to lower coverage, which suggests that nothing happened after flashing the sample to 452 K except for molecular desorption.

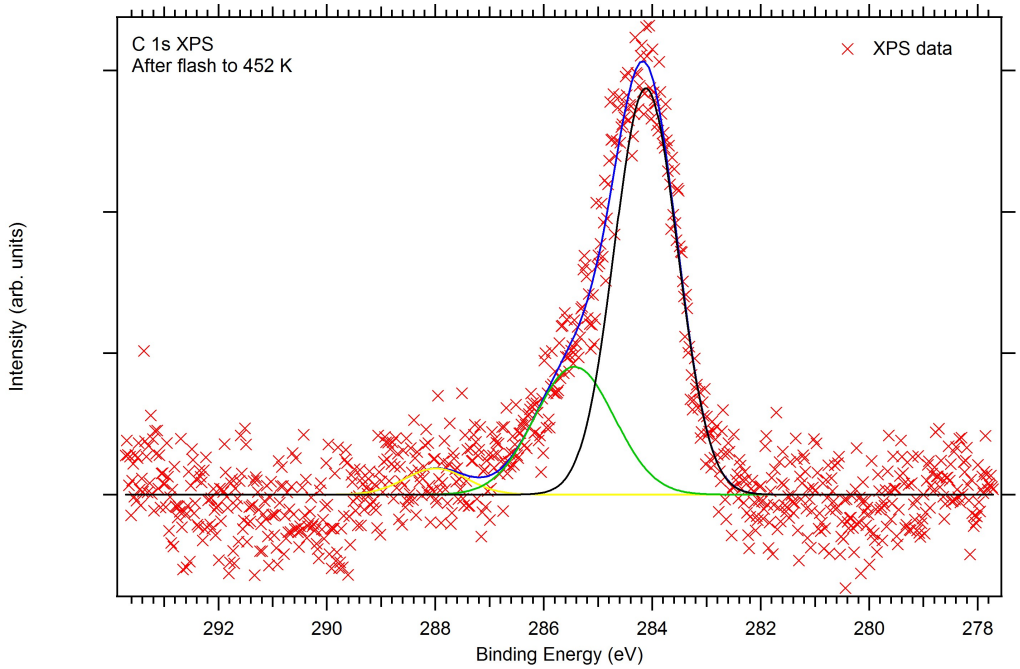

Figure 19: XPS spectrum of C 1s. After flashing the sample to 452 K the intensity ratio were distorted, but the binding energies were essentially the same. Peak one shifted 0.17 EV towards higher binding energy.

In figure 20 a C 1s spectrum after flashing the sample to 701 K is shown. One can see that it has changed compared to earlier spectra; according to ref. [18] the molecules have changed to benzoate. A change into benzoate will result in two C 1s peaks, but as seen in figure 20 we still have three peaks. Also, a large decrease in intensity is seen, simply the result of desorption. Figure 21 shows the different C 1s spectra obtained at different conditions. In table 3 the experimental values are attributed and compared to the literature values.

Table 2: Table of binding energies obtained by fitting Gauss functions to XPS spectra of C 1s with different coverage and after flashing to different temperatures

Spectrum	BE peak 1(eV)	Γ 1(eV)	BE peak 2(eV)	Γ 2(eV)	BE peak 3(eV)	Γ 3(eV)
100 L Styrene	287.87	0.81	285.44	1.04	284.16	0.82
1000 L Styrene	287.83	0.81	285.43	1.04	284.22	0.82
Flash 452 K	287.99	0.81	285.43	1.04	284.12	0.82
Flash 701 K	287.06	0.81	284.74	1.04	283.98	0.82

According to ref. [4] desorbing styrene molecules will leave strongly bound C atoms, even after annealing to 900 K. Ref. [21] states that a C 1s peak of 283.8 eV originates from pre-experiment C. Binding energies of residual C and pre-experiment C should be the same. Therefore the peak at 283.98

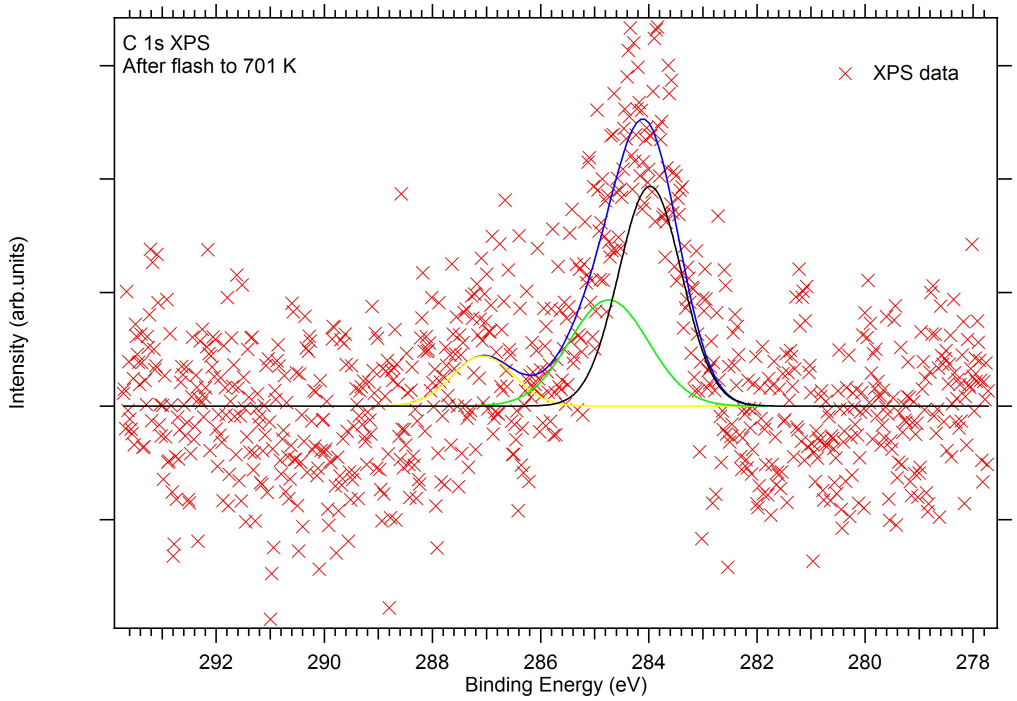

Figure 20: XPS spectra of C1s after flash to 701 K. The C1s peaks has shifted as a effect of the flash.

is attributed to residual C. Studies in ref. [18] suggest that the rest of the carbon may originate from benzene. Solomon et al. [22] recorded x-ray photoelectron spectra of benzene adsorbed on Ag(110) and attributed a C 1s peak with binding energy 284.7 eV to benzene. This suggests that the peak at 284.74 eV has its origin in benzene, which is supported by ref. [2] that also obtained 284.7 eV. All benzene should have desorbed during the flash, the fact that there still is a fair amount of C present at the surface even after the flash to 701 K is surprising. The flash may not have been sufficient to desorb the C. One can conclude that benzene is strongly bound to the clusters.

In ref. [18] the carboxylic groups in benzoate were found to have a binding energy of 287.4 eV, which is slightly higher than the value obtained after

Table 3: Attributed binding energies compared with literature values.

Reaction intermediate	Experiment values (eV)	Literature values (eV)
Residual C	283.98	283.8
Phenyl ring	284.12-284.22	284.2
Benzene	284.74	284.7
Oxametallacycle	285.43-285.44	285.6, 285.7
Benzoate carboxyl	-	287.4
Strongly bound carboxylic groups	287.06	287.9
Carboxylic groups	287.83-287.99	287.9

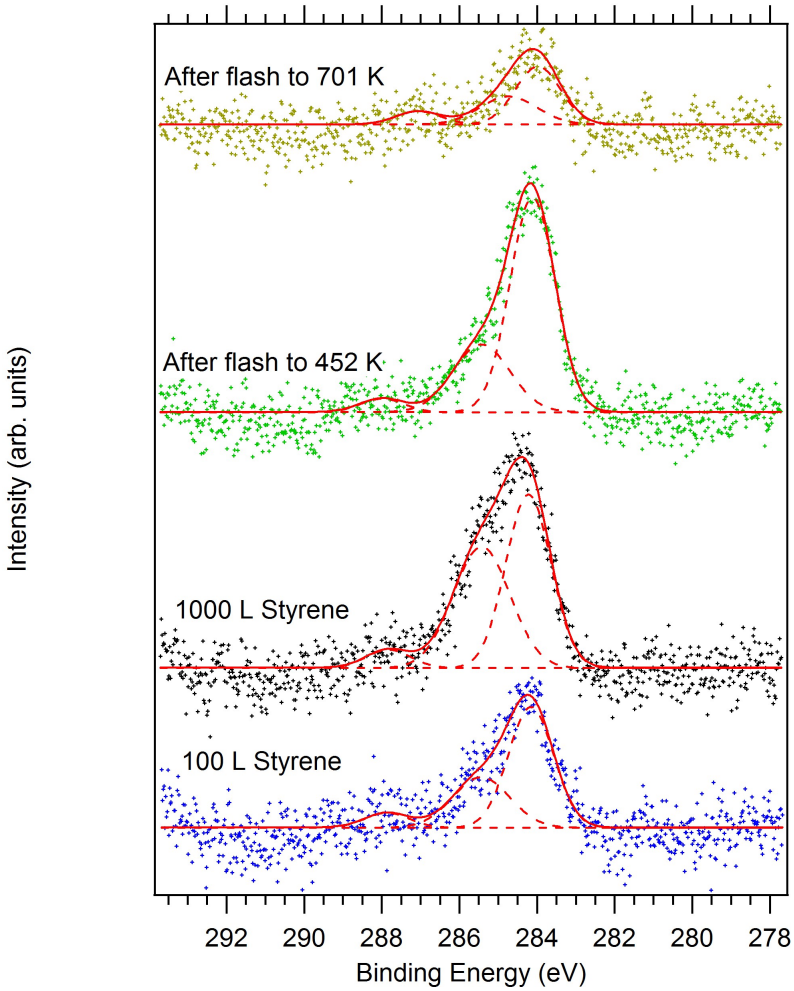

Figure 21: Different C1s spectra taken at different times. One can see the shifts corresponding to structural changes. Solid lines are the fit function and dashed lines the individual peaks.

flashing to 701 K. The associated phenyl ring has a binding energy of 284.2 eV [2] which was not detected. The absence of a peak with a binding energy characteristic of phenyl suggests that it is a clean carboxylic group. Therefore peak 1 may be attributed to a carboxylic group. By comparing with earlier values for carboxylic groups, see table 3, the postflash carboxylic groups underwent a large shift. This implies that the carboxylic groups is strongly bound to the carbon clusters.

It is clear that oxidized Ag clusters on a FeO film with a Pt substrate can be used for styrene epoxidation. The reaction pathway suggested by ref. [2] appears to be valid, as seen in fig. 2. All the reaction intermediates cannot be observed. Benzoate is not detected in this experiment. However, both carboxylic groups and benzene are seen, suggesting that benzoate has

disassociated. The disassociation of benzoate into benzene and CO_2 is shown in ref. [18], but there in gas phase. It seems like this surface disassociates styrene into three parts: residual C, carboxylic groups, and benzene. The three fragments then binds strongly to the clusters. It is good to notice that these three fragments are the molecular components of styrene.

XPS alone is not sufficient to investigate styrene epoxidation. Using this technique one will only be able to probe the fragments absorbed on the surface before and after the reaction. By not being able to see the gas phase reactants, much information is unseen. Complementary methods are needed, such as high pressure photoelectron spectroscopy (HPXPS). Using HPXPS one would be able to probe gas phase molecules at the surface, as well as the reaction itself. By being able to study the reaction itself, at the correct pressure, fundamental information about the reaction mechanisms may be found.

6 Summary

Ethene epoxidation is an important chemical reaction. With an ethene production of 18 million metric tons a year, it is important to understand the mechanisms behind epoxidation. X-ray photoelectron spectroscopy is a good technique for investigating surface properties, but one must conduct these experiments in UHV. To perform epoxidation of ethene in UHV, low temperatures are required due to the low adsorption. It has been found that styrene is a good substitute to ethene when performing epoxidation studies, and in addition, styrene epoxidation in itself is also a very important chemical reaction. Here a surface consisting of a Pt(111) substrate has been used, upon the substrate a FeO(111) film was grown. Upon the FeO(111) film, silver clusters were deposited and oxidized.

The film was created by depositing and oxidizing Fe on the Pt(111) substrate. After the FeO(111) film was complete, Ag was deposited on the surface and formed clusters. Oxygen was dosed on the surface to oxidize the clusters. After dosing different amounts of styrene, the oxametallacycle was detected. It was also possible to identify the phenyl ring attached as well as a carboxyl group. When flashing the sample the molecular structure changed. It was found that styrene had changed into carboxylic groups, benzene and carbon residuals. The reaction path suggested by ref. [2] seems to be accurate.

It is possible to use silver as a heterogeneous catalyst for styrene epoxidation. The surface used in this experiment has successfully replicated the reaction path seen together with styrene epoxidation. One cannot definitely say that styrene was epoxidized because no gas phase molecules could be detected with the setup. It was also found that the surface used seems to disassociate styrene into benzene, carboxylic groups, and C residuals, which are the components needed to create styrene.

Acknowledgments

I gratefully acknowledge the help received from J. Knudsen, J. Schnadt and C. Isvoranu during the experiment at MAX-Lab. I would like tho thank J. Schnadt for supervising me through this project. Also, I would like to thank the department of synchrotron radiation research at Lund University for letting me do my bachelor thesis at their division.

References

[1] H.-J. Leeetal., Chemical Engineering Science 65, 2010, 128-134

[2] L. Zhou, R.J. Madix, J. Phys. Chem. C 112, 2008, 4725-4734

[3] F.J. Williams et al. J. Phys. Chem. B 107, 2003, 3824-3828

[4] A. Klust, R.J. Madix, Surface Science 600, 2006, 5025-5040

[5] W. Weiss, W. Ranke, Progress in Surface Science 70, 2002, 1-151

[6] V.J. Inglezakis, S.G. Poulopoulos, Adsorption, Ion Exchange and Catalysis, Elsevier, 2006

[7] S. Hüfner, Photoelectron Spectroscopy, Second edition, Springer, Berlin, 1996

[8] G. Attard, C. Barnes, Surfaces, Oxford univ. Press, 1998

[9] S. Svanberg, Atomic and Molecular Spectroscopy, Forth edition, Springer, Berlin, 2004

[10] Å. Andersson et al. Nucl. Instr. and Meth. in Phys. Res. A 343, 1994, 644-649

[11] C. Kittel, Introduction to Solid State Physics, Eighth edition, Wiley, Hoboken, 2005

[12] H. Ibach, H. Lüth, Solid-State Physics, Fourth edition, Springer, Berlin, 2009

[13] R. Nyholm et al. Nuclear Instruments and Methods in Physics Research A 467-468, 2001, 520-524

[14] S. Ismat Shaha et al. Handbook of Deposition Technologies for Films and Coatings, Chapter 4, Third Edition, Elsevier, 2009

[15] D. Depla S. Mahieu, J.E. Greene Handbook of Deposition Technologies for Films and Coatings, Chapter 5, Third Edition, Elsevier, 2009

[16] G. Panaccione et al., C. R. Physique 9, 2008, 524-536

[17] MAX-Lab: http://www.maxlab.lu.se/beamlines/bli311/images/Resolution2.JPG, 100517

[18] L. Zhou, R.J. Madix, Surface Science 603, 2009, 1751-1755

[19] A. Klust, R.J. Madix, J.AM. Chem. Soc. 128, 2006, 1034-1035

[20] M.A. Langell, Surface Science 320, 1994 25-38

[21] A.A. Dias et al., Vacuum 64, 2002, 445-450

[22] J.L. Solomon et al. Surface Science 255, 1991, 12-30